



## OPEN ACCESS

EDITED BY  
He Xiaojun,  
Wenzhou Medical University, China

REVIEWED BY  
Yuna Qian,  
University of Chinese Academy of  
Sciences, China  
Hong Chen,  
Luoyang Normal University, China

\*CORRESPONDENCE  
Hongcai Guan,  
1687875577@qq.com

<sup>†</sup>These authors have contributed equally  
to this work

SPECIALTY SECTION  
This article was submitted to Medicinal  
and Pharmaceutical Chemistry,  
a section of the journal  
Frontiers in Chemistry

RECEIVED 12 August 2022  
ACCEPTED 03 October 2022  
PUBLISHED 28 October 2022

CITATION  
Zheng H, Huang Z, Chen T, Sun Y,  
Chen S, Bu G and Guan H (2022),  
Gallium ions incorporated silk fibroin  
hydrogel with antibacterial efficacy for  
promoting healing of *Pseudomonas*  
*aeruginosa*-infected wound.  
*Front. Chem.* 10:1017548.  
doi: 10.3389/fchem.2022.1017548

COPYRIGHT  
© 2022 Zheng, Huang, Chen, Sun,  
Chen, Bu and Guan. This is an open-  
access article distributed under the  
terms of the [Creative Commons  
Attribution License \(CC BY\)](https://creativecommons.org/licenses/by/4.0/). The use,  
distribution or reproduction in other  
forums is permitted, provided the  
original author(s) and the copyright  
owner(s) are credited and that the  
original publication in this journal is  
cited, in accordance with accepted  
academic practice. No use, distribution  
or reproduction is permitted which does  
not comply with these terms.

# Gallium ions incorporated silk fibroin hydrogel with antibacterial efficacy for promoting healing of *Pseudomonas aeruginosa*-infected wound

Hui Zheng<sup>1†</sup>, Zhida Huang<sup>1†</sup>, Tongxin Chen<sup>2</sup>, Yafeng Sun<sup>1</sup>,  
Shouqing Chen<sup>1</sup>, Guangming Bu<sup>2</sup> and Hongcai Guan<sup>1\*</sup>

<sup>1</sup>Wenzhou Institute of Industry & Science, Wenzhou, Zhejiang, China, <sup>2</sup>Ruibang Laboratories, Wenzhou, Zhejiang, China

The continual resistance to antibiotics and the generation of a series of bacterial infections has emerged as a global concern, which requires appropriate measures and therapeutics to address such a menace. Herein, we report on Silk fibroin (SF) hydrogel with good biocompatibility and biodegradability fabricated through the crosslinking of the SF of different concentrations with Gallium nitrate (Ga (NO<sub>3</sub>)<sub>3</sub>) against *Pseudomonas aeruginosa*. However, the SF: Ga = 500: 1 (w/w) (SF/Ga) demonstrated a good bactericidal and wound healing effect as a result of the moderate and prolonged release of the Ga<sup>3+</sup> following the gradual degradation of the hydrogel. The Ga<sup>3+</sup>, known for its innovative nature acted as a crosslinked agent and a therapeutic agent employing the “Trojan horse” strategy to effectively deal with the bacteria. Also, the Ga<sup>3+</sup>, which is positively charged neutralizes the negative potential value of the SF particles to reduce the charge and further induce the β-sheet formation in the protein structure, a characteristic of gelation in SF. The morphology showed a fabricated homogenous structure with greater storage modulus- G' with low loss modulus- G'' modulus demonstrating the mechanical performance and the ability of the SF/Ga hydrogel to hold their shape, at the same time allowing for the gradual release of Ga<sup>3+</sup>. A demonstration of biocompatibility, biodegradability, bactericidal effect and wound healing in *in vitro* and *in vivo* present the SF/Ga hydrogel as an appropriate platform for therapeutic and for antibacterial wound dressing.

## KEYWORDS

silk fibroin protein, gallium, hydrogels, against bacterial, wound healing

## Introduction

On the one hand, bacterial infections have been on the rise as a result of the uncertain resistance generated by the bacteria following the administration of antibiotics. A condition that has largely been attributed to the misuse and continual use of these antibiotics. As a consequence of these more than 14 million individuals are affected each year and continue to be affected with a substantial rise in the case of morbidity and mortality (Wang et al., 2017). On the other hand, and to a great degree, skin injuries occurring from diverse conditions make the body vulnerable to this bacterial infection and even dehydration (Wu et al., 2019; Yu et al., 2022). Therefore, the upkeeping of an organism's first line of defense from invasion by microorganisms and even homeostasis easily becomes compromised (Zhou et al., 2018; He et al., 2020). All these present the need for a suitable cause of action for the treatment of bacterial infections and rapid means of managing wounds.

Employing polymeric hydrogel owing to its soft tissue-like hydrophilic properties has recently gained prominence when it comes to wound-related cases (Kirker et al., 2002; Mogoşanu and Grumezescu, 2014). Therein, the silk fibroin (SF) a natural protein polymer extracted from the cocoons of the silkworm, *Bombyx mori* have also been extensively studied due to their waterproof nature, biodegradability, gaseous permeation, mild inflammatory potential and homeostatic properties (Minoura et al., 1995; Santin et al., 1999; Gil et al., 2013). These properties allow the SF to easily coordinate between bacteria strains and the antibacterial substance they are reinforced with, thus perfect for antibacterial and wound dressing. Additionally, the modification of the physical parameters of SF aqueous solution, pH, conditions for sonication, and dehydration *via* the addition of ethanol or polymer can trigger the transformation of SF molecules from random-coil/ $\alpha$ -helix structures to  $\beta$ -sheets, boosting the physical crosslinking (Hu et al., 2013; Bai et al., 2014; Kambe and Yamaoka, 2019). It is worth noting that, the formation of  $\beta$ -sheets triggers the sol-gel transition of silk fibroin through hydrophobic interaction of molecules, which results in the stabilization of hydrogels (Matsumoto et al., 2006; Nultsch and Germershaus, 2017). Though the influence of mechanical forces and pH on the SF has been extensively studied, the role of ions in the SF hydrogels remains poorly understood. Kelly and co-workers reported that some amino acid residues can emerge as  $\beta$ -turns through chelation with copper ions and subsequently form stable  $\beta$ -sheet by hydrogen bonding (Schneider and Kelly, 1995). Also, some studies show that the folding process of the SF may easily be affected by some ions such as  $\text{Ca}^{2+}$ ,  $\text{Zn}^{2+}$ ,  $\text{K}^+$ , and  $\text{Na}^+$  (Zhou et al., 2004; Zong et al., 2004; Ruan et al., 2008; Ruan and Zhou, 2008). These studies illustrated that the suitable ions may have the ability to induce the sol-gel transition of silk fibroin.

What's more, one crucial nutrient required by the bacteria for the coordination of DNA synthesis, cellular respiration and even eluding of the destructive activity through the generation of ROS is iron (Fe) (Andrews et al., 2003; Hijazi et al., 2018). On the contrary,  $\text{Ga}^{3+}$  is an anti-infective agent capable of binding to biological complexes containing Fe due to the resemblance in chemical properties, permitting their infiltration into such essential  $\text{Fe}^{3+}$  binding sites within protein and enzymes. Consequently, this process can alter the Fe content in the bacteria's antioxidant enzymes disrupting the redox-driven process and making the bacteria susceptible to oxidants (Bernstein, 1998; Lemire et al., 2013; Goss et al., 2018; Wang et al., 2019).  $\text{Ga}(\text{NO}_3)_3$  has been reported to have a highly significant bactericidal effect against *P. aeruginosa* even at as low concentrations and is not reduced under physiological conditions (Kaneko et al., 2007; Minandri et al., 2014; Chitambar, 2016). However, no prior research has been reported on the influence of the  $\text{Ga}^{3+}$  on the SF. In this study, SF:  $\text{Ga}(\text{III})$  hydrogels were synthesized through the electrostatic adherence of  $\text{Ga}(\text{NO}_3)_3$  into SF with different concentrations to form a new type of antibacterial hydrogel with ideal mechanical properties and for the first time, we report on the effect against the *P. aeruginosa* and for wound healing. The effect of the SF:  $\text{Ga}(\text{III}) = 500: 1$  (w/w) (SF/ $\text{Ga}$ ) was investigated *in vitro* and *in vivo*. Positively charged  $\text{Ga}^{3+}$  could "kill two birds with one stone", in addition to antibacterial action, it cause the aggregation of fibroin molecules into hydrophilic regions, forming a SF hydrogel through ionic crosslinks. The SF/ $\text{Ga}$  hydrogel exhibited a highly effective antibacterial efficiency capacity in the *in vitro* with good biocompatibility. This was confirmed by the *in vivo* experiments where the SF/ $\text{Ga}$  hydrogel effectively disrupted the *P. aeruginosa* *via* the slowly and prolonged release of the  $\text{Ga}^{3+}$  at the same time stepping up with the wound recovery. In all, SF/ $\text{Ga}$  hydrogel demonstrate great potential for treating bacterial infections and wound dressing.

## Experiment section

### Materials

*Bombyx mori* cocoons were provided by Chongqing University (China). Gallium nitrate hydrate (99.9% metals basis) was purchased from MACKLIN. Sodium carbonate ( $\text{Na}_2\text{CO}_3$ ), Boric acid, and Sodium chloride ( $\text{NaCl}$ ) were purchased from Sigma. Lithium Bromide salt ( $\text{LiBr}$ ), sodium hydroxide ( $\text{NaOH}$ ) were purchased from Aladdin. Tryptone Broth was purchased from Sangon Biotech. Dialysis bag (MD44, 3.5 K MWCO) was purchased from Solarbio. CCK-8 was purchased from APE×BIO, and DMEM was purchased from Life Technologies Corporation.

## Preparation of silk fibroin solution

*Bombyx mori* cocoons were degummed to remove sericin proteins; silk cocoons were treated in alkaline water baths (0.02 mol/L  $\text{Na}_2\text{CO}_3$ ) at 100°C for 2 h. Degummed silk was washed several times in deionized water and dried at room temperature to obtain pure SF fibers. The dried SF was dissolved in 9.3 mol/L LiBr solution and stirred for 1 h at 65°C. After cooling, the solution was taken out into a dialysis bag, placed in an alkaline buffer solution (Boric acid 18.54 g, NaCl 8.775 g dissolved in 1 L of deionized water, pH titration to 9) dialyzed for 1 day to remove the LiBr salt. The solution was dialyzed against deionized water for 3 days and subsequently filtered. At last, pure SF aqueous solution was obtained, and the final concentration was about 5% (w/v), which was stored at 4°C.

## Determination of MIC value of gallium nitrate on *P. aeruginosa*

Using a 96-well plate, the half-dilution method was used to obtain 128  $\mu\text{g/ml}$  to 1  $\mu\text{g/ml}$   $\text{Ga}(\text{NO}_3)_3$  solution of 50  $\mu\text{L}$  per well, and 50  $\mu\text{L}$  of *P. aeruginosa* bacterial solution with the value of  $\text{OD}_{600} = 0.05$  added to each well. The plate was incubated at 37°C in a constant temperature incubator for 24 h.  $\text{OD}_{600}$  value was measured with a microplate reader (Thermo scientific).

## Preparation of silk fibroin-gallium nitrate hydrogel

The SF: Ga (III) hydrogels were prepared by mixing  $\text{Ga}(\text{NO}_3)_3$  with SF in solution. The SF solution and  $\text{Ga}(\text{NO}_3)_3$  were mixed in different ratios for use, specifically, the SF solution concentration was maintained at 5% by changing the blend volume ratio, and the mass ratios of SF and  $\text{Ga}(\text{NO}_3)_3$  were 5000:1, 2500:1, 1000:1, 500:1 and 250:1, which were ultrasonicated for 1 h after mixing, and the state of gelation observed after standing. Based on the gel formation time and properties, SF: Ga(III) = 500: 1 (w/w) is expected to be the best ratio.

## SEM and EDS characterizations

The scanning electron microscope (SEM; HITACHI SU8010, Japan) was used to analyze the dried gel morphology. The SF hydrogel and SF/Ga hydrogel were quickly frozen in liquid nitrogen for 10 min, and after, placed in a vacuum freeze dryer (BIOCOOL, China) and freeze-dried at -50°C for 72 h. The sample was pasted on the round sample stage with a conductive double-sided adhesive. Before the test, the sample was processed with gold spray. The thickness of the gold spray

was between 20 and 30 nm, and the test was conducted at a temperature of 20°C and relative humidity of 65%.

## CD and FTIR characterizations

CD spectra of samples were measured on an Applied Photophysics (Chirascan Plus, England) spectrometer under an  $\text{N}_2$  atmosphere. Approximately 20  $\mu\text{L}$  of the samples were evenly placed on a 1 mm thick quartz cuvette and scanned from 180 to 260 nm. Three groups of samples (SF solution, SF solution after 1 h of ultrasound, SF solution, and  $\text{Ga}(\text{NO}_3)_3$ ) were mixed at a mass ratio of 500:1. The samples for the Fourier transform infrared spectrometer (FTIR, Bruker Tensor II, Germany) were also freeze-dried. The wave number range was 2000–1000  $\text{cm}^{-1}$ , the spectral resolution was 4  $\text{cm}^{-1}$ , and the scanning range was 4000–400  $\text{cm}^{-1}$ .

## Rheological test

The mechanical and rheological analyses were carried out using (TA Instrument, New Castle, DE). The elasticity (storage modulus-  $G'$ ) and viscosity (loss modulus-  $G''$ ) were evaluated at a shear frequency of 1 Hz within a linear viscoelastic region. All frequency sweeps were collected within a frequency range of 0.1–10 Hz rad/s at 25°C. All samples were stabilized and measured, and the process was repeated three times.

## Zeta potential

The samples [Mixed  $\text{Ga}(\text{NO}_3)_3$  with SF solution (0.05% wt) at 1000:1, 500:1 (w/w), and SF solution only] were characterized with a nanometer particle size analyzer (Malvern, Zetasizer Nano ZS ZEN3600, England) to determine the change of Zeta potential, and each sample was measured three times repeatedly.

## Cell culture and cytotoxicity assay

Human lung fibroblasts (MRC-5) cells were cultured in DMEM medium supplemented with 100 U  $\text{ml}^{-1}$  penicillin, 0.1  $\text{mg ml}^{-1}$  streptomycin, and 10% FBS at 37°C in a humidified incubator under 5%  $\text{CO}_2$ . After reaching 80% confluence, cells were harvested and seeded in 96-well plates ( $2 \times 10^4$  cells/well). At the same time, 1 ml PBS solution, SF, and SF/Ga hydrogel were separately put into the 6-well plate, sterilized under UV for 30 min and 5 ml DMEM, was added to each well for co-cultivation. After 24 h, the culture medium was replaced with hydrogel leaching solution for each group and cells were cultured for 1 day. The cytotoxicity was measured by the CCK-8 method.

## Antibacterial property

The antibacterial activities of the SF/Ga hydrogel against *P. aeruginosa* bacteria were evaluated using the oscillation method. LB culture medium was used to dilute *P. aeruginosa* solution which was recovered for 24 h,  $OD_{600} = 0.05$ . The bacterial solutions (4 ml) were added to 15 ml shake tubes and later divided into 3 groups: 1 ml of SF hydrogel, SF/Ga hydrogel, and  $Ga(NO_3)_3$  solution. The samples were cultured in a 37°C constant temperature incubator, and Shaked for 7 days. The samples (100  $\mu$ L) were taken out every day and the  $OD_{600}$  was measured.

## Wound healing

To evaluate the potential of the SF/Ga hydrogel for wound dressing, an *in vivo* experiment was conducted using a rat model with a *P. aeruginosa*-infected wound. (He et al., 2022a; He et al., 2022b). Six 3-month-old healthy Sprague–Dawley (SD) rats were randomly divided into 2 groups (PBS and SF/Ga hydrogel treatments) and anesthetized with chloral hydrate. The back fur of the mice was shaved, cleaned, and disinfected with 75% alcohol and an 8-mm biopsy punch was used to create circular wounds of full thickness, 8 mm in diameter on each rat. The wounds were infected with 100  $\mu$ L of  $10^8$  CFU/mL *P. aeruginosa* solution. Images of the wound area at 0, 1, 2, 3, and 6 days were taken with a digital camera, and the percentage of wound size was calculated using ImageJ software.

## Statistical analysis

All the experiments were performed with sample sizes greater than three, and the experimental results were expressed as the mean value  $\pm$  standard deviation. The difference between the groups was determined using a one-way analysis of variance, and a *p*-value smaller than 0.05 was considered a statistically significant difference.

## Result and discussion

### Susceptibility of *P. aeruginosa* to $Ga(NO_3)_3$

The release of  $Ga^{3+}$  is not able to appropriately replace the  $Fe^{3+}$  within the protein binding site of bacteria since the  $Ga^{3+}$  transition to  $Ga^+$  requires much energy compared to the transition of Fe electrons from 3 + to 2 + or *vice versa* (Ma et al., 2013; Nikolova et al., 2016; Best et al., 2020). Hence the disruption of the crucial processes by  $Ga^{3+}$  after replacing the  $Fe^{3+}$  and the subsequent antibacterial action. The susceptibility of *P. aeruginosa* was investigated to screen the concentration of Ga

$(NO_3)_3$  used in the SF: Ga (III) hydrogel fabrication. As shown in Figure 1A, the Minimum inhibition concentration (MIC) of  $Ga(NO_3)_3$  was recorded as 16  $\mu$ g/ml which was sufficient to completely disrupt the *P. aeruginosa*. Also, a measure of the toxicity of the different concentrations of  $Ga(NO_3)_3$  on the human lung fibroblast (MRC) using the MTT assay, Figure 1B showed that an increment in the concentration of  $Ga(NO_3)_3$  from 16  $\mu$ g/ml to 1024  $\mu$ g/ml yielded cell viability which was above 80%. This indicated the negligible toxicity of the concentration of  $Ga(NO_3)_3$  within this interval.

## Preparation of the SF: Ga (III) hydrogels

The SF: Ga (III) hydrogels were successfully fabricated after sonication for 1 h and standing for 23 h to form a hydrogel with increased stability, the presence of amino and carboxyl groups allowed for the easy chemical modification. Thus, the addition of  $Ga(NO_3)_3$  solution of varying concentrations (12.5  $\mu$ g, 25  $\mu$ g, 50  $\mu$ g, 100  $\mu$ g, and 200  $\mu$ g) and the subsequent induction of the gelation of the mixed solution *via* sonication, Figure 2A. The even dispersion of  $Ga(NO_3)_3$  within the SF formed a hydrogel network SF: Ga (III) resulting from the self-crosslinking. As shown in, Figure 2B, the uniform dispersion allowed SF: Ga (III) to release bioactive  $Ga^{3+}$  at the same time providing a moist environment and enough mechanical support while holding their shapes. The antibacterial effect and the gelation time led to the selection of the 100  $\mu$ g/ml,  $Ga(NO_3)_3$ , combined with the SF hydrogel to give SF: Ga (III) = 500: 1 (w/w) (SF/Ga), Figure 2C. The time for the gelation is dependent on the concentration of the gelatine and gel strength also significantly increases with an increase in the gelation concentration. Considering the varying ratio of SF: Ga (III), gelation was expected to decrease from the highest concentration (5000–250) to the lowest with time. However, on average the hydrogels demonstrated a shorter gelation time. Hence, a positive correlation in SF/Ga with their crosslinking and other physical properties.

## Morphological analysis of the SF/Ga hydrogel

A high proportion of the SF is bound to increase the viscosity of the hydrogel solution, inducing a short gelation time which can restrict the crosslinking and at the same time affect the porosity (Xu et al., 2021). The SEM evaluation of the influence of  $Ga(NO_3)_3$  on the micromorphological structure of the hydrogel after dried freezing revealed a lamellar interconnected pores size for SF hydrogel, Figure 3A, and a smaller but increased pore size for  $Ga(NO_3)_3$  crosslinked hydrogel SF/Ga, Figure 3B. In all, the morphological evaluation shows the hydrogel was three-dimensionally porous. Elemental analysis of SF/Ga hydrogels with an X-ray energy spectrometer (EDS) attached to the high-

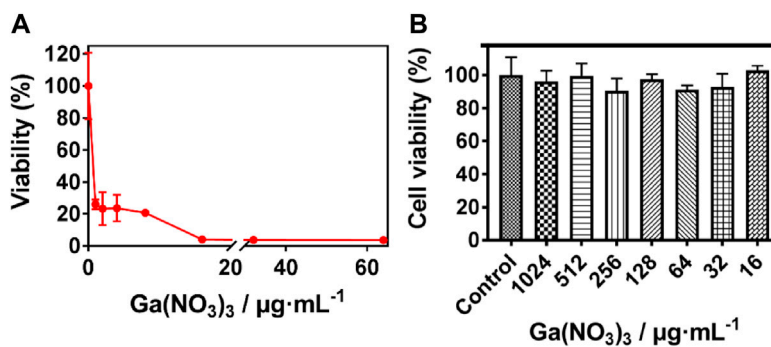


**FIGURE 1**  
Susceptibility of *P. aeruginosa* to  $\text{Ga}(\text{NO}_3)_3$ . (A) Minimum inhibition concentration of  $\text{Ga}(\text{NO}_3)_3$  against *P. aeruginosa*, (B) Cytotoxicity of  $\text{Ga}(\text{NO}_3)_3$  to MRC-5 (mean  $\pm$  SD,  $n = 3$ ).

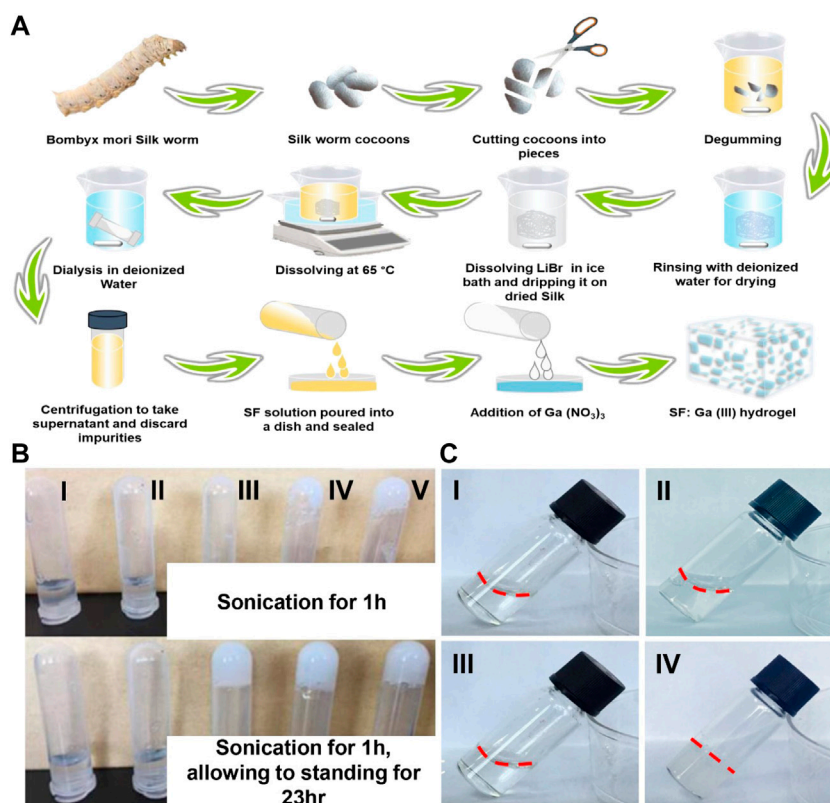


**FIGURE 2**  
Synthesis of hydrogels. (A) Schematic illustration of the preparation of SF and SF: Ga(III) hydrogels, (B) Digital images of (I) SF: Ga(III) = 5000: 1 (w/w), (II) SF: Ga(III) = 2500: 1 (w/w), (III) SF: Ga(III) = 1000: 1 (w/w), (IV) SF: Ga(III) = 500: 1 (w/w) (SF/Ga) and (V) SF: Ga(III) = 250: 1 (w/w) hydrogels, (C) Digital image of SF solution (I, II) and SF: Ga(III) = 500: 1 (w/w) (SF/Ga) hydrogel (III, IV) before and after sonication and standing for 23 h.

resolution electron microscope, confirmed the presence of C, N, O, and Ga elements in the fabricated SF/Ga hydrogel, where C, N, and O are components of silk fibroin and, Ga a mixed component

of  $\text{Ga}(\text{NO}_3)_3$ , **Figure 3C**. The changes in the protein secondary structure of the SF/Ga were explored using circular dichroism (CD) and compared with those of unsonicated SF solution and

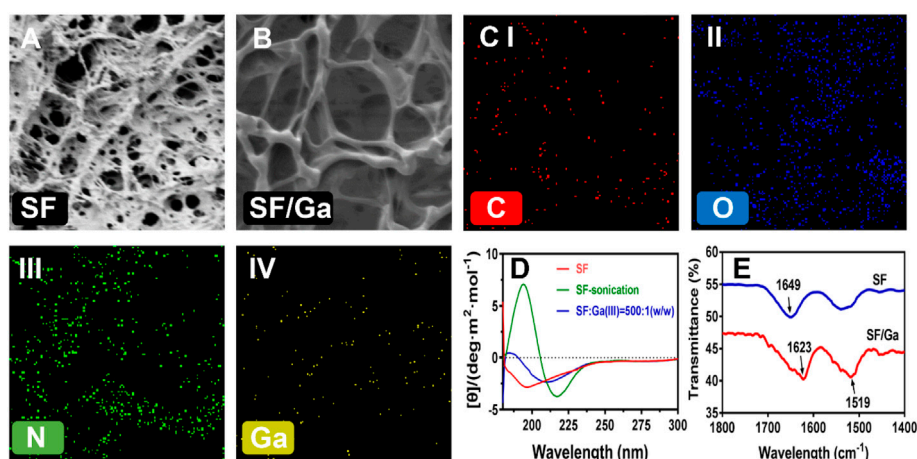


FIGURE 3

Morphological and secondary structural characterization. (A,B) SEM images of the surface pore of SF and SF/Ga hydrogel, (C) Elemental mapping of SF/Ga hydrogel, (D) CD spectrum of unsonicated SF, ultrasonicated SF, and sonicated SF/Ga solutions, (E) FTIR of SF and SF/Ga hydrogel.

ultrasonicated SF within 180–260 nm. As shown in Figure 3D, CD spectrum of the unsonicated SF solutions revealed a negative intensity peak close to 195 nm, this indicates a typical random coil structure. In addition, the CD spectrum of the sonicated SF solution showed a negative and positive intensity peak at 217 nm and 198 nm respectively, which is more typical of a characteristic peak within  $\beta$ -sheet conformation. Interestingly addition of Ga ( $\text{NO}_3$ )<sub>3</sub> to the SF demonstrated a change that accompanied the SF/Ga switching from a random coil structure to a  $\beta$ -sheet conformation which was consistent with the change in the conformation of the SF after adding Ga ( $\text{NO}_3$ )<sub>3</sub>. Emphasizing that the  $\beta$ -sheet is the dominant secondary structure in the SF/Ga. Figure 3E shows the FTIR spectra which investigated the interaction between Ga ( $\text{NO}_3$ )<sub>3</sub> and the SF, and this reveals a spectra peak of amide I (1700–1600  $\text{cm}^{-1}$ ) and amide II (1600–1500  $\text{cm}^{-1}$ ) regions for the SF. The SF conformation comprises a random coil,  $\alpha$ -helix,  $\beta$ -sheet, and  $\beta$ -turn. A characteristic peak with the interval of 1625–1640  $\text{cm}^{-1}$  (amide I) and 1515–1525  $\text{cm}^{-1}$  (amide II) indicated that the secondary structure is related to the  $\beta$ -sheet. Similarly, the peaks of 1640–1660  $\text{cm}^{-1}$  (amide I) and 1535–1550  $\text{cm}^{-1}$  (amide II) indicated that the secondary structure of the protein is dominated by the  $\alpha$ -helix and random coil. However, peaks identified at 1700–1600  $\text{cm}^{-1}$  (amid I) and amide II (1600–1500  $\text{cm}^{-1}$ ) of SF represented relative maturity. Figure 3E, also showed that 1649  $\text{cm}^{-1}$ , 1625  $\text{cm}^{-1}$ , and 1519  $\text{cm}^{-1}$  are characteristic absorption peaks of SF amide I, amide I, and amide II, respectively, indicating that pure silk fibroin has a random coil structure. But the addition of Ga ( $\text{NO}_3$ )<sub>3</sub> to the SF, shifted the position of the characteristic peak of the SF to the right, that is, it changed to the silk II conformation, showing an antiparallel  $\beta$ -sheet. Hence, the  $\beta$ -sheet structure is a

significant characteristic of SF, giving SF a good mechanical property. This also shows the successful incorporation of Ga ( $\text{NO}_3$ )<sub>3</sub> in the SF/Ga hydrogel.

## Mechanical and rheological properties of SF/Ga

Some reports indicate that the  $\beta$ -sheet is directly responsible for a silk hydrogel mechanical property as a result of improved crosslinks (Hu et al., 2010; Guzewicz et al., 2011; Xu et al., 2021). Hence crosslinking coordinates and improves the mechanical performance of a hydrogel further enabling resistance to easy deformation (Rammensee et al., 2006; Zawko et al., 2009; Jeon et al., 2014). The influence of Ga ( $\text{NO}_3$ )<sub>3</sub> on the SF hydrogels and the viscosity difference were evaluated *via* a dynamic oscillatory rheological measurement of the storage modulus-  $G'$  and loss modulus-  $G''$  of sample SF and SF/Ga against time and frequency. Mechanical spectra of SF and SF/Ga showed that the storage modulus-  $G'$  highly exceeded the loss modulus-  $G''$ . An indication of a well-obtained hydrogel network, Figures 4A,B. However, a time sweep at a frequency of 1 Hz showed that the SF/Ga had significant stability compared to the SF which could be attributed to Ga ( $\text{NO}_3$ )<sub>3</sub> concentration and the presence of the  $\beta$ -sheet conformation from the cross-linking. The Zeta potential is the magnitude of change that determines the stability of a colloidal suspension. As shown in Figure 4C, the SF revealed a negative Zeta potential value of about -30 mV. However, an increase in the content of Ga ( $\text{NO}_3$ )<sub>3</sub> in the hydrogel significantly decreases the value of the Zeta potential. An indication of possible electrostatic adsorption between the positively charged  $\text{Ga}^{3+}$ , of Ga ( $\text{NO}_3$ )<sub>3</sub>, and the negatively charged SF.

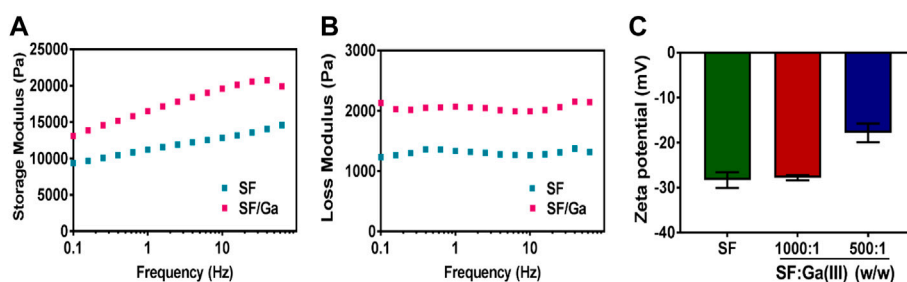


FIGURE 4 (A,B) Rheological characterization and (C) Zeta-potentials (B) of SF and SF/Ga hydrogel (mean  $\pm$  SD,  $n = 3$ ).

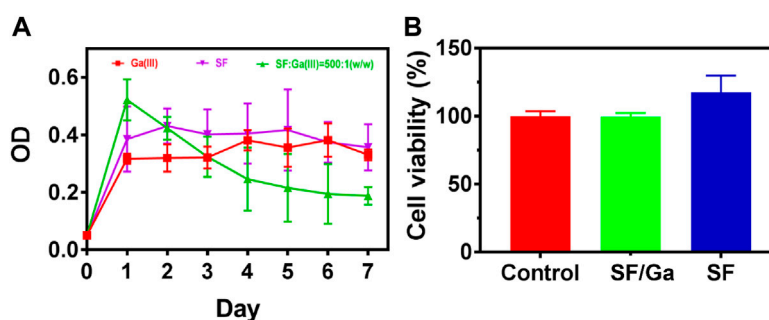


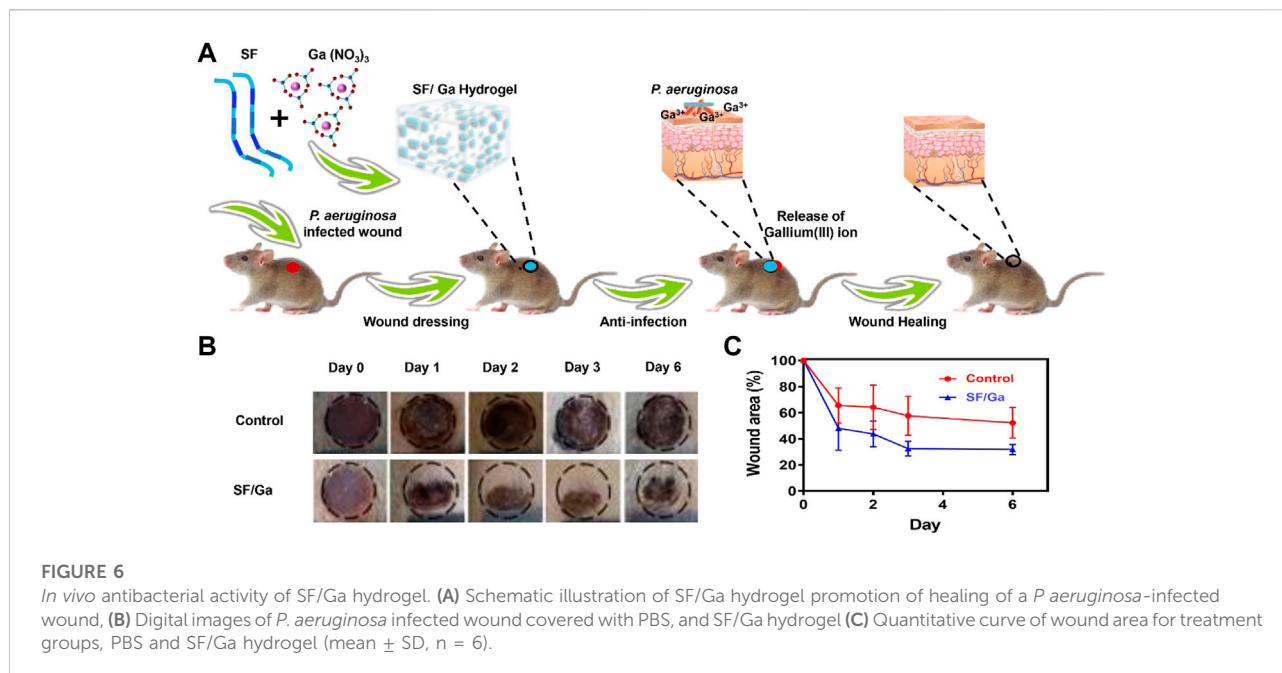
FIGURE 5 *In vitro* antibacterial activity (A) and biocompatibility (B) of SF/Ga hydrogel (mean  $\pm$  SD,  $n = 3$ ).

Also, this demonstrated that the configuration of the SF and SF: Ga (III) = 1000: 1 (w/w) were random coils, whereas the neutralization process by the positively charged  $\text{Ga}^{3+}$  yielded a  $\beta$ -sheet in the SF/Ga.

### *In vitro* antibacterial activity and biocompatibility

Gallium compounds have been employed in many areas in the biomedical field for the treatment of many infectious diseases and even in cancer treatment (Rudnev et al., 2006; Rzhepishevskaya et al., 2011; Deliormanli, 2015). Thus, we investigated the antibacterial efficiency of the SF/Ga against *P. aeruginosa*. The effect of 100  $\mu\text{g}/\text{mL}$   $\text{Ga}(\text{NO}_3)_3$  solution, 50 mg/ml pure SF solution, and SF/Ga on the growth of *P. aeruginosa* showed a lower OD value for  $\text{Ga}(\text{NO}_3)_3$  group compared to the SF/Ga group and a high OD value for the SF group, Figure 5A. The significant antibacterial activity observed in  $\text{Ga}(\text{NO}_3)_3$  could be attributed to the release of  $\text{Ga}^{3+}$  while the high OD value in the SF hydrogel group, indicated the insignificant antibacterial effect. Results from the second day showed the gradual degradation of

the hydrogel in the SF/Ga group with a gradual decline in the OD value. The gradual decline in the OD value demonstrated the gradual release of  $\text{Ga}^{3+}$  as the hydrogel gradually degrades. Extension of time to the 7th day demonstrated a significantly reduced OD value in the SF/Ga group compared to the other two groups. Intriguingly a critical observation of the OD value showed that the bacteria suspension in the  $\text{Ga}(\text{NO}_3)_3$  group began to rise steadily from the 3rd day. This can be ascribed to the hydrolysis of  $\text{Ga}(\text{NO}_3)_3$  which reduces the activity of  $\text{Ga}(\text{NO}_3)_3$  and permitted the bacteria regrowth. This also proves the SF/Ga hydrogel can present a prolonged and efficient antibacterial effect. Also, apart from the antibacterial activity, biocompatibility serves as a direct prerequisite for a biomedical purposes. The *in vitro* cytocompatibility was examined using human lung fibroblast (MRC -5) cells in a CCK-8 assay. As shown in Figure 5B, cells inoculated with SF and SF/Ga hydrogels leaching solution for 24 h demonstrated a cell activity of about 100% relative to the control group, indicating negligible cytotoxicity. However, cells in the SF hydrogels group demonstrated an obvious cell proliferation effect. SF/Ga hydrogel proves good biocompatibility with an efficient antibacterial effect.



## In vivo antibacterial activity

The result from the *in vitro* antibacterial activity and biocompatibility inspired us to further investigate the *in vivo* antibacterial activity of SF/Ga hydrogel. A *P. aeruginosa* infection model in the SD rats was created by making skin incisions on the back of the rats, PBS solution, and SF/Ga hydrogel were applied separately, Figure 6A. The wound recovery in the control group was very slow. In contrast, the SF/Ga group demonstrated a better and more pronounced wound recovery effect Figure 6B. Images of wounds taken at a separate time interval from 0,1,2,3 to 6 days showed that the wound treated with SF/Ga hydrogel exhibited a wound area of about 70% relative to the control group on the 3rd day, an indication of the release of  $\text{Ga}^{3+}$  for bactericidal effect in the SF/Ga group and with time the wound size began to decrease Figure 6C. On the 6th day, the wound scar rate and closure of the wound in the SF/Ga group were observed to be better compared to the other group, indicating the SF/Ga hydrogel which contains  $\text{Ga}(\text{NO}_3)_3$  wielded the potential to effectively disrupt bacterial activity and at the same time accelerating the wound healing process. This confirms results from the *in vitro* antibacterial activity and presents SF/Ga as an appropriate biomaterial for antibacterial effects and wound healing.

## Conclusion

In summary, we successfully prepared SF/Ga hydrogel and systematically investigated the therapeutic and wound healing ability against *P. aeruginosa*. The SF/Ga hydrogel showed a good water content, biocompatibility, mechanical strength, and

biodegradability. The hydrogel allowed the gradual and prolonged release of  $\text{Ga}^{3+}$  which in turn gradually disrupted the bacteria. Besides SF/Ga hydrogel demonstrated negligible toxicity towards human lung fibroblast (MRC-5) cells affirming their biocompatibility. More importantly, the SF/Ga hydrogel effect on *P. aeruginosa* infected wound exhibited effective recovery confirming its ability to disrupt bacteria and at the same time induce wound healing. Therefore SF/Ga hydrogel can serve as an excellent multifunctional candidate for wound dressing with a prolonged antibacterial effect.

## Data availability statement

The original contributions presented in the study are included in the article/supplementary materials, further inquiries can be directed to the corresponding author.

## Ethics statement

The animal study was reviewed and approved by Animal Ethics Association of Wenzhou Institute of Industry & Science.

## Author contributions

Credit Author Statement HZ and ZH: Conceptualization, Methodology, Software. GB: Data curation, Writing-Original draft preparation. YS: Visualization, Investigation. HG: Supervision, Funding acquisition, Project administration. SC:



Software, Validation. TC, HZ, and HG: Writing—Reviewing and Editing.

## Funding

This work was financially supported by Wenzhou Science and Technology Plan Project (ZG2021035).

## Conflict of interest

Authors TC and GB were employed by Ruibang Laboratories.

## References

- Andrews, S. C., Robinson, A. K., and Rodríguez-Quiñones, F. (2003). Bacterial iron homeostasis. *FEMS Microbiol. Rev.* 27, 215–237. doi:10.1016/s0168-6445(03)00055-x
- Bai, S., Zhang, X., Lu, Q., Sheng, W., Liu, L., Dong, B., et al. (2014). Reversible hydrogel–solution system of silk with high beta-sheet content. *Biomacromolecules* 15, 3044–3051. doi:10.1021/bm500662z
- Bernstein, L. R. (1998). Mechanisms of therapeutic activity for gallium. *Pharmacol. Rev.* 50, 665–682.
- Best, M. G., Cunha-Reis, C., Ganin, A. Y., Sousa, A., Johnston, J., Oliveira, A. L., et al. (2020). Antimicrobial properties of gallium(III)- and iron(III)-Loaded polysaccharides affecting the growth of *Escherichia coli*, *Staphylococcus aureus*, and *Pseudomonas aeruginosa*, in vitro. *ACS Appl. Bio Mater.* 3, 7589–7597. doi:10.1021/acsbm.0c00811
- Chitambar, C. R. (2016). Gallium and its competing roles with iron in biological systems. *Biochimica Biophysica Acta - Mol. Cell Res.* 1863, 2044–2053. doi:10.1016/j.bbamcr.2016.04.027
- Deliormanli, A. M. (2015). Synthesis and characterization of cerium- and gallium-containing borate bioactive glass scaffolds for bone tissue engineering. *J. Mater. Sci. Mater. Med.* 26, 1–13.
- Gil, E. S., Panilaitis, B., Bellas, E., and Kaplan, D. L. (2013). Functionalized silk biomaterials for wound healing. *Adv. Healthc. Mater.* 2, 206–217. doi:10.1002/adhm.201200192
- Goss, C. H., Kaneko, Y., Khuu, L., Anderson, G. D., Ravishankar, S., Aitken, M. L., et al. (2018). Gallium disrupts bacterial iron metabolism and has therapeutic effects in mice and humans with lung infections. *Sci. Transl. Med.* 10, eaat7520. doi:10.1126/scitranslmed.aat7520
- Guziewicz, N., Best, A., Perez-Ramirez, B., and Kaplan, D. L. (2011). Lyophilized silk fibroin hydrogels for the sustained local delivery of therapeutic monoclonal antibodies. *Biomaterials* 32, 2642–2650. doi:10.1016/j.biomaterials.2010.12.023
- He, X., Dai, L., Ye, L., Sun, X., Enoch, O., Hu, R., et al. (2022). A vehicle-free antimicrobial polymer hybrid gold nanoparticle as synergistically therapeutic platforms for *Staphylococcus aureus* infected wound healing. *Adv. Sci.* 9, 2105223. doi:10.1002/advs.202105223
- He, X., Hou, J.-T., Sun, X., Jangili, P., An, J., Qian, Y., et al. (2022). NIR-II photo-amplified sonodynamic therapy using sodium molybdenum bronze nanoplatform against subcutaneous *Staphylococcus aureus* infection. *Adv. Funct. Mat.* 32, 2203964. doi:10.1002/adfm.202203964
- He, X., Liu, X., Yang, J., Du, H., Chai, N., Sha, Z., et al. (2020). Tannic acid-reinforced methacrylated chitosan/methacrylated silk fibroin hydrogels with multifunctionality for accelerating wound healing. *Carbohydr. Polym.* 247, 116689. doi:10.1016/j.carbpol.2020.116689
- Hijazi, S., Visaggio, D., Pirolo, M., Frangipani, E., Bernstein, L., and Visca, P. (2018). Antimicrobial activity of gallium compounds on ESKAPE pathogens. *Front. Cell. Infect. Microbiol.* 8, 316. doi:10.3389/fcimb.2018.00316
- Hu, X., Lu, Q., Sun, L., Cebe, P., Wang, X., Zhang, X., et al. (2010). Biomaterials from ultrasonication-induced silk Fibroin–Hyaluronic acid hydrogels. *Biomacromolecules* 11, 3178–3188. doi:10.1021/bm1010504
- Hu, X., Tang-Schomer, M. D., Huang, W., Xia, X. X., Weiss, A. S., and Kaplan, D. L. (2013). Charge-tunable autoclaved silk-tropoelastin protein alloys that control neuron cell responses. *Adv. Funct. Mat.* 23, 3875–3884. doi:10.1002/adfm.201202685
- Jeon, O., Samorezov, J. E., and Alsberg, E. (2014). Single and dual crosslinked oxidized methacrylated alginate/PEG hydrogels for bioadhesive applications. *Acta biomater.* 10, 47–55. doi:10.1016/j.actbio.2013.09.004
- Kambe, Y., and Yamaoka, T. (2019). Biodegradation of injectable silk fibroin hydrogel prevents negative left ventricular remodeling after myocardial infarction. *Biomater. Sci.* 7, 4153–4165. doi:10.1039/c9bm00556k
- Kaneko, Y., Thoendel, M., Olakanmi, O., Britigan, B. E., and Singh, P. K. (2007). The transition metal gallium disrupts *Pseudomonas aeruginosa* iron metabolism and has antimicrobial and antibiofilm activity. *J. Clin. Invest.* 117, 877–888. doi:10.1172/jci30783
- Kirker, K. R., Luo, Y., Nielson, J. H., Shelby, J., and Prestwich, G. D. (2002). Glycosaminoglycan hydrogel films as bio-interactive dressings for wound healing. *Biomaterials* 23, 3661–3671. doi:10.1016/s0142-9612(02)00100-x
- Lemire, J. A., Harrison, J. J., and Turner, R. J. (2013). Antimicrobial activity of metals: Mechanisms, molecular targets and applications. *Nat. Rev. Microbiol.* 11, 371–384. doi:10.1038/nrmicro3028
- Ma, H., Darmawan, E. T., Zhang, M., Zhang, L., and Bryers, J. D. (2013). Development of a poly(ether urethane) system for the controlled release of two novel anti-biofilm agents based on gallium or zinc and its efficacy to prevent bacterial biofilm formation. *J. Control. Release* 172, 1035–1044. doi:10.1016/j.jconrel.2013.10.005
- Matsumoto, A., Chen, J., Collette, A. L., Kim, U.-J., Altman, G. H., Cebe, P., et al. (2006). Mechanisms of silk fibroin Sol–Gel transitions. *J. Phys. Chem. B* 110, 21630–21638. doi:10.1021/jp056350v
- Minandri, F., Bonchi, C., Frangipani, E., Imperi, F., and Visca, P. (2014). Promises and failures of gallium as an antibacterial agent. *Future Microbiol.* 9, 379–397. doi:10.2217/fmb.14.3
- Minoura, N., Aiba, S.-I., Higuchi, M., Gotoh, Y., Tsukada, M., and Imai, Y. (1995). Attachment and growth of fibroblast cells on silk fibroin. *Biochem. biophysical Res. Commun.* 208, 511–516. doi:10.1006/bbrc.1995.1368
- Mogoşanu, G. D., and Grumezescu, A. M. (2014). Natural and synthetic polymers for wounds and burns dressing. *Int. J. Pharm.* 463, 127–136. doi:10.1016/j.ijpharm.2013.12.015
- Nikolova, V., Angelova, S., Markova, N., and Dudev, T. (2016). Gallium as a therapeutic agent: A thermodynamic evaluation of the competition between Ga<sup>3+</sup> and Fe<sup>3+</sup> ions in metalloproteins. *J. Phys. Chem. B* 120, 2241–2248. doi:10.1021/acs.jpcc.6b01135
- Nultsch, K., and Germershaus, O. (2017). Silk fibroin degumming affects scaffold structure and release of macromolecular drugs. *Eur. J. Pharm. Sci.* 106, 254–261. doi:10.1016/j.ejps.2017.06.012
- Rammensee, S., Hümmerich, D., Hermanson, K. D., Scheibel, T., and Bausch, A. R. (2006). Rheological characterization of hydrogels formed by recombinantly produced spider silk. *Appl. Phys. A* 82, 261–264. doi:10.1007/s00339-005-3431-x
- Ruan, Q. X., Zhou, P., Hu, B. W., and Ji, D. (2008). An investigation into the effect of potassium ions on the folding of silk fibroin studied by generalized two-dimensional NMR–NMR correlation and Raman spectroscopy. *FEBS J.* 275, 219–232. doi:10.1111/j.1742-4658.2007.06191.x

The remaining authors declare that the research was conducted in the absence of any commercial or financial relationships that could be construed as a potential conflict of interest.

## Publisher's note

All claims expressed in this article are solely those of the authors and do not necessarily represent those of their affiliated organizations, or those of the publisher, the editors and the reviewers. Any product that may be evaluated in this article, or claim that may be made by its manufacturer, is not guaranteed or endorsed by the publisher.

- Ruan, Q. X., and Zhou, P. (2008). Sodium ion effect on silk fibroin conformation characterized by solid-state NMR and generalized 2D NMR–NMR correlation. *J. Mol. Struct.* 883–884, 85–90. doi:10.1016/j.molstruc.2007.11.055
- Rudnev, A. V., Foteeva, L. S., Kowol, C., Berger, R., Jakupec, M. A., Arion, V. B., et al. (2006). Preclinical characterization of anticancer gallium(III) complexes: Solubility, stability, lipophilicity and binding to serum proteins. *J. Inorg. Biochem.* 100, 1819–1826. doi:10.1016/j.jinorgbio.2006.07.003
- Rzhapishevska, O., Ekstrand-Hammarström, B., Popp, M., Björn, E., Bucht, A., Sjöstedt, A., et al. (2011). The antibacterial activity of Ga<sup>3+</sup> is influenced by ligand complexation as well as the bacterial carbon source. *Antimicrob. Agents Chemother.* 55, 5568–5580. doi:10.1128/aac.00386-11
- Santin, M., Motta, A., Freddi, G., and Cannas, M. (1999). In Vitro Evaluation of the Inflammatory Potential of the Silk Fibroin. *J. Biomed. Mater. Res.* 46, 382–389.
- Schneider, J. P., and Kelly, J. W. (1995). Templates that induce .alpha.-Helical, beta.-sheet, and loop conformations. *Chem. Rev.* 95, 2169–2187. doi:10.1021/cr00038a015
- Wang, Y., Han, B., Xie, Y., Wang, H., Wang, R., Xia, W., et al. (2019). Combination of gallium(iii) with acetate for combating antibiotic resistant *Pseudomonas aeruginosa*. *Chem. Sci.* 10, 6099–6106. doi:10.1039/c9sc01480b
- Wang, Z., Dong, K., Liu, Z., Zhang, Y., Chen, Z., Sun, H., et al. (2017). Activation of biologically relevant levels of reactive oxygen species by Au/g-C<sub>3</sub>N<sub>4</sub> hybrid nanozyme for bacteria killing and wound disinfection. *Biomaterials* 113, 145–157. doi:10.1016/j.biomaterials.2016.10.041
- Wu, J., Chen, A., Zhou, Y., Zheng, S., Yang, Y., An, Y., et al. (2019). Novel H<sub>2</sub>S-Releasing hydrogel for wound repair via *in situ* polarization of M2 macrophages. *Biomaterials* 222, 119398. doi:10.1016/j.biomaterials.2019.119398
- Xu, Z., Chen, T., Zhang, K. Q., Meng, K., and Zhao, H. (2021). Silk fibroin/chitosan hydrogel with antibacterial, hemostatic and sustained drug-release activities. *Polym. Int.* 70, 1741–1751. doi:10.1002/pi.6275
- Yu, Y., Yang, B., Tian, D., Liu, J., Yu, A., and Wan, Y. (2022). Thiolated hyaluronic acid/silk fibroin dual-network hydrogel incorporated with bioglass nanoparticles for wound healing. *Carbohydr. Polym.* 288, 119334. doi:10.1016/j.carbpol.2022.119334
- Zawko, S. A., Suri, S., Truong, Q., and Schmidt, C. E. (2009). Photopatterned anisotropic swelling of dual-crosslinked hyaluronic acid hydrogels. *Acta Biomater.* 5, 14–22. doi:10.1016/j.actbio.2008.09.012
- Zhou, P., Xie, X., Knight, D. P., Zong, X. H., Deng, F., and Yao, W. H. (2004). Effects of pH and calcium ions on the conformational transitions in silk fibroin using 2D Raman correlation spectroscopy and <sup>13</sup>C solid-state NMR. *Biochemistry* 43, 11302–11311. doi:10.1021/bi049344i
- Zhou, Q., Kang, H., Bielec, M., Wu, X., Cheng, Q., Wei, W., et al. (2018). Influence of different divalent ions cross-linking sodium alginate-polyacrylamide hydrogels on antibacterial properties and wound healing. *Carbohydr. Polym.* 197, 292–304. doi:10.1016/j.carbpol.2018.05.078
- Zong, X. H., Zhou, P., Shao, Z. Z., Chen, S. M., Chen, X., Hu, B. W., et al. (2004). Effect of pH and copper(II) on the conformation transitions of silk fibroin based on EPR, NMR, and Raman spectroscopy. *Biochemistry* 43, 11932–11941. doi:10.1021/bi049455h